Geometrical Improvements of Rotational Stabilization of High-n Ballooning Modes in Tokamaks

M. Furukawa,[1] S. Tokuda,[1] and M. Wakatani [2]

[1] Naka Fusion Research Establishment, JAERI, Naka, Ibaraki 311-0193, Japan
[2] Graduate School of Energy Science, Kyoto University, Gokasho, Uji 611-0011, Japan

E-mail: furukawm@fusion.naka.jaeri.go.jp

Abstract. We have found numerically that damping phases appear in the time evolution of the perturbation energy of high-n ballooning modes in the presence of toroidal shear flows. The damping dominates exponential growth which occurs in the bad curvature region, resulting in stabilization of ballooning modes. D-shaping of plasma cross-section, reduction of aspect ratio, and arrangement of X-point at inner side of the torus enhance the stabilization effect of the toroidal flow through this mechanism.

1 Introduction

The edge localized modes (ELMs) [1] in the H-mode [2] tokamak plasmas are the magnetohydrodynamic (MHD) activity. Type-I (giant) ELM is related to ideal MHD ballooning modes or peeling modes [1, 3]. At the edge region of the tokamak, the plasma often rotates. The rotation is considered to affect the MHD stability.

The WKB theory for high-n ideal MHD ballooning modes was developed by Connor, Hastie and Taylor [4]. Introduction of Doppler shift in the eikonal representation for the perturbation enables us study of high-n ballooning modes for toroidally rotating tokamaks [5–9]. It was shown that the high-n ballooning equations including toroidal flows have dynamical symmetry, and the solutions can exhibit periodically modulated exponential growth. Numerical solutions for the Shafranov equilibrium were shown in Ref. [10], and the unstable region in the so-called S–α diagram was shown to shrink by the toroidal flow shear.

However, the mechanism of stabilization for ballooning modes by the toroidal flow shear has not been fully clarified. If the flow shear is very small, then ballooning perturbation is considered to evolve as in a static plasma with a given ballooning angle θ_k at each instance. This leads to an expression of the growth rate in a rotating plasma; $\gamma = \int_{-\pi}^{\pi} \gamma^{\rm st} {\rm d}\theta_k / 2\pi$, where $\gamma^{\rm st}$ is the growth rate in a static plasma and is a function of θ_k [10]. However, if $\gamma^{\rm st} > 0$ for any θ_k; i.e., pressure gradient exceeds its critical value in a static plasma, $\gamma > 0$ since $\gamma^{\rm st} \geq 0$ in the ideal MHD model. Then the system cannot be stabilized. Therefore we have studied the mechanism of stabilization numerically, and found that the perturbation energy damps owing to the flow shear. The damping occurs in the good curvature region. When the damping dominates the exponential growth in the bad curvature region, the ballooning mode is stabilized. Thus, the stabilization of ballooning modes by the toroidal flow shear is expected to be enhanced by the reduction of (i) the instantaneous growth rate and (ii) the duration of the exponentially growing phase. In this paper we control them by changing geometrical parameters such as aspect ratio, ellipticity, triangularity, and position of X-point. We found numerically that D-shaping, reduction of aspect ratio, and arrangement of X-point at inner side of the torus enhance the stabilization effect of the toroidal flow. In Section 2, the physical mechanism of stabilization is clarified. In Section 3, the sensitivity to the geometrical parameters such as aspect ratio, ellipticity, triangularity, and position of X-point are investigated. Conclusions are given in Section 4.

2 Mechanism of Stabilization

We obtain MHD equilibria by solving the Grad-Shafranov equation including toroidal flows [13] numerically under semi-fixed boundary condition. The pressure profile has a large gradient near the plasma edge. The poloidal beta is $\beta_{\rm P} = 1.2$ for equilibria with the aspect ratio $A = 3$, and the ratio $\beta_{\rm P}/A = 0.4$ is fixed when A is varied to keep the Shafranov shift. The current density profile is slightly modified from a parabola to adjust the safety factor $q = 5$ at the 95% flux surface. We have investigated the stability on the 95% flux surface, which is 3–5cm inner from the separatrix when the minor radius is 1m. The total plasma current is adjusted so that $q = 1$ at the magnetic axis. As for the toroidal flow, the flow shear can be given arbitrarily on a magnetic surface since the flow shear does not contribute to the force balance as long as the magnitude of the flow itself is zero. Thus the toroidal rotation frequency Ω is zero in the equilibrium calculations. Finally, when a magnetic-shear parameter $s_{\rm m}$ and a pressure-gradient parameter $\alpha_{\rm p}$ are varied on a magnetic surface, we have used the local equilibrium of Greene and Chance [14].

First we show in Fig. 1 the time evolution of $\|\xi_\perp^2\|$ and $\|\xi_\parallel^2\|$ for the aspect ratio $A = 3$, the ellipticity $\kappa = 1.4$, the triangularity $\delta = 0.4$, the magnetic shear parameter $s_{\rm m} = 3$, the pressure gradient parameter $\alpha_{\rm p} = 3.4$, and toroidal flow shear $\Omega'\tau_{\rm A} = -0.03$, where $\|a\| \equiv \int a {\rm d}\vartheta$, ϑ is the poloidal angle in the covering space, and $\tau_{\rm A}$ is the Alfvén time (connection length/Alfvén velocity). The prime denotes the derivative with respect to the normalized poloidal flux. The value of $\Omega'\tau_{\rm A} = -0.03$ is achieved in conventional tokamak experiments [15]. In National Spherical Torus Experiment (NSTX), $\Omega'\tau_{\rm A} \simeq -0.3$ is obtained [16]. The horizontal axis denotes time normalized by the period $\tau_{\rm d} \equiv 2\pi/({\rm d}\Omega/{\rm d}q)$. The vertical line at $t/\tau_{\rm d} = 1$ and 2 indicates the timings when the phases of each twisted slice mode are the same at $\theta = 0$ (bad curvature side) [9].

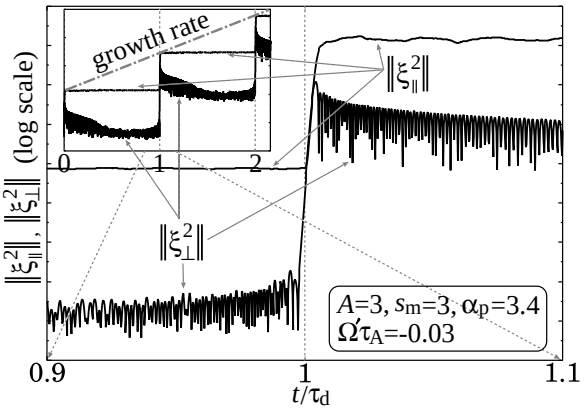

FIG. 1. Time evolution of $\|\xi_\perp^2\|$ and $\|\xi_\parallel^2\|$. When the phases of each twisted slice mode are the same at $\theta = 0$, $\|\xi_\perp^2\|$ grows exponentially.

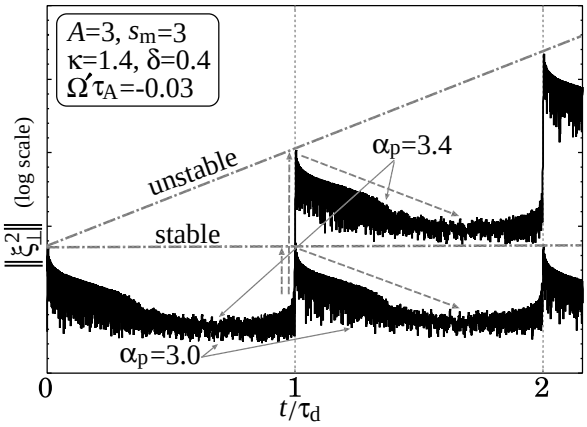

FIG. 2. Time evolution of $\|\xi_\perp^2\|$ for $\alpha_{\rm p} = 3.0$ (stable) and 3.4 (unstable). Stability is determined by the competition between the exponential growth and the damping of $\|\xi_\perp^2\|$.

We found from Fig. 1 that damping phases appear in the time evolution of $\|\xi_\perp^2\|$. The damping is the crucial mechanism for the stabilization due to the flow shear. We also found that $\|\xi_\perp^2\|$ grows around $t/\tau_{\rm d} = 1, 2, \cdots$, and $\|\xi_\parallel^2\|$ begins to grow after $\|\xi_\perp^2\|$ becomes sufficiently large. If $\|\xi_\perp^2\|$ does not increase on the average over the time period, then $\|\xi_\parallel^2\|$ oscillates rather than grows or

damps. The instantaneous growth rate is nearly equal to the growth rate in the static plasma. As for the time duration of the exponentially growing phase, it is very short in Fig. 1, since the unstable region in the θ_k space is narrow in the static plasma. Thus $\|\xi_\perp^2\|$ is closely related to the driving mechanism of the instability, and therefore we focus on it in the following.

In Fig. 2, the time evolution of $\|\xi_\perp^2\|$ is shown for $\alpha_\mathrm{p} = 3.0$ and 3.4. The flow shear is $\Omega'\tau_\mathrm{A} = -0.03$. We found that the damping of $\|\xi_\perp^2\|$ dominates the exponential growth at $t/\tau_\mathrm{d} = 1, 2, \cdots$ for $\alpha_\mathrm{p} = 3.0$, and the ballooning mode is stabilized. For $\alpha_\mathrm{p} = 3.4$, on the other hand, the damping is not strong enough to dominate the exponential growth. The competition between the damping and the growth determines the stability of the ballooning mode in the presence of the toroidal shear flow.

Therefore, we expect that the stabilization of ballooning modes by a flow shear could be further enhanced by reduction of (i) the instantaneous growth rate and (ii) the duration of the exponentially growing phase. In the next Section, we verify it by changing geometrical parameters such as aspect ratio A, ellipticity κ, triangularity δ, and position of X-point.

3 Improved Stability by Geometrical Effects

3.1 D-shaping and Aspect Ratio

First, we change the ellipticity and triangularity while keeping the magnetic curvature at the outer side of the torus unchanged. This means the driving force of ballooning modes; i.e., the product of the pressure gradient and the magnetic curvature, is held constant. Figure 3 shows the time evolution of $\|\xi_\perp^2\|$ for circular cross-section and D-shaped tokamaks. The aspect ratio is $A = 3$ and the flow shear is $\Omega'\tau_\mathrm{A} = -0.03$. The instantaneous growth rate at the exponentially growing phase is almost the same for the two equilibria. Here, $\alpha_\mathrm{p} = 1.8$ for the circular cross-section, and $\alpha_\mathrm{p} = 3.8$ for the D-shape. These equilibria are located near the first stability boundary in the S–α diagram. Thus if α_p is the same, the instantaneous growth rate is smaller in the D-shaped tokamak plasma. The reason is known as the increase of the good curvature region. As for the duration of the exponentially growing phase, we found that it is shorter for the D-shape, since the good curvature region is wider than that for the circular cross-section. This leads to enhancement of the stabilization effect of the flow shear.

Figure 4 shows the critical pressure gradient $\alpha_\mathrm{p}^\mathrm{crit}$ as a function of triangularity δ. To keep the magnetic curvature at the outer side of the torus unchanged, κ and δ are changed simultaneously; (κ, δ)=(1,0), (1.2,0.2), (1.4,0.4), and (1.6,0.6). We found, from Fig. 4, that the increment of $\alpha_\mathrm{p}^\mathrm{crit}$ due to the flow shear increases as δ. Therefore, the D-shaping not only raises the critical pressure gradient of ballooning modes in a static plasma, but also enhances the stabilization effect of toroidal flow shear. This is favorable for tokamaks aiming at high beta.

Next, we change the aspect ratio. As in the case of D-shaping, the reduction of the aspect ratio increases good curvature region on a magnetic field line. In Fig. 5, the critical pressure gradient $\alpha_\mathrm{p}^\mathrm{crit}$ is shown as a function of A. As A is reduced, $\alpha_\mathrm{p}^\mathrm{crit}$ increases in both static and rotating plasmas. The increment of $\alpha_\mathrm{p}^\mathrm{crit}$ due to the flow shear also increases as A is reduced. Thus the reduction of A is favorable to achieve high beta plasmas.

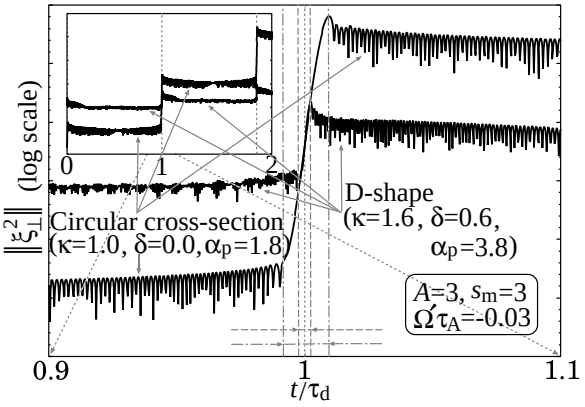

FIG. 3. Time evolution of $\|\xi_\perp^2\|$ for circular cross-section and D-shaped tokamaks. The time duration of the exponential growth is shorter for the D-shaped tokamak. The instantaneous growth rate at the exponential growth is almost the same, although α_p is significantly larger for the D-shaped tokamak.

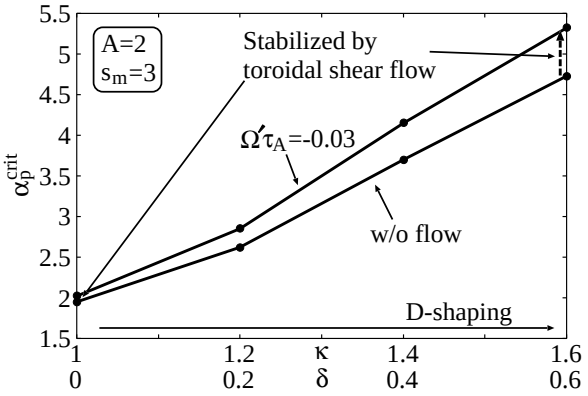

FIG. 4. Sheared toroidal rotation raises the critical pressure gradient α_p^{crit}. The increase of α_p^{crit} becomes more remarkable by D-shaping, which is favorable for tokamaks aiming at high beta.

3.2 Position of X-point

It is known that a magnetic field line stays for much of its length in the vicinity of the X-point, and the local shear is divergent. Therefore ballooning/interchange stability was studied for model [17] and JT-60U [18] equilibria with an X-point, and it was shown that an X-point at the outer side of the torus does not change first stability boundary significantly [18].

In the present paper, we include a toroidal shear flow, since the mechanism of stabilization of ballooning modes by the flow shear is closely related to the magnetic configuration. We have examined ballooning stability of two extremely different equilibria; one has an X-point at the inner side of the torus, and the other has at the outer side. The aspect ratio of both equilibria is $A = 10$ and the beta is very low, thus the cross-sectional shape is nearly circular except for the region close the separatrix. These are not realistic, however, the difference of magnetic configuration due to the X-point is magnified.

We show the growth rate $\gamma\tau_A$ as a function of flow shear $\Omega'\tau_A$ in Fig. 6. The growth rate without a flow is 0.2 for both equilibria. In the equilibrium with inside X-point, the ballooning mode is stabilized by a smaller $\Omega'\tau_A$ than in the equilibrium with outside X-point. We have also calculated α_p^{crit} and its increase by a flow shear ($\Omega'\tau_A = -0.03$) for the separatrix equilibria, however, the first stability boundary is not affected largely. The reason is conjectured as follows. In a static equilibrium, growth rate of ballooning mode becomes significantly large at α_p slightly larger than its marginal value around the first stability boundary. Thus a small flow shear cannot affect its growth significantly.

4 Conclusions

We have clarified the mechanism of stabilization of high-n ballooning modes by toroidal flow shear numerically. Damping phases appear in the time evolution of the perturbation. The damping dominates the exponential growth in the bad curvature region, which leads to the stabilization of the ballooning modes. D-shaping and reduction of aspect ratio enhance the stabilization

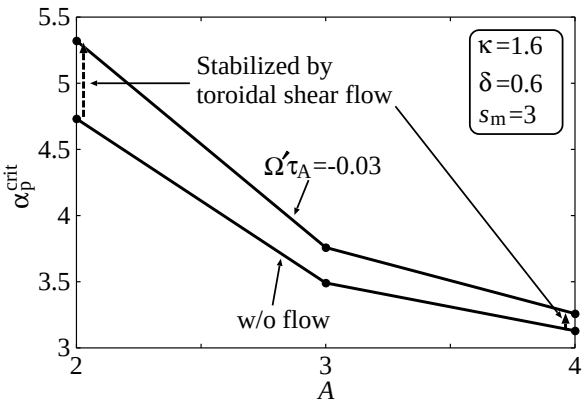

FIG. 5. Reduction of aspect ratio increases not only α_p^{crit} in a static plasma, but also the increment of α_p^{crit} due to the toroidal flow shear.

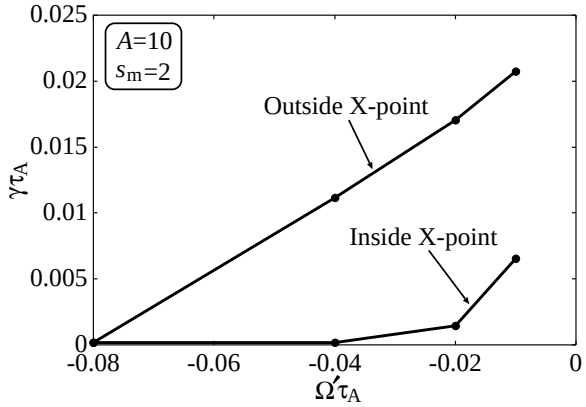

FIG. 6. Growth rate $\gamma\tau_A$ is plotted as a function of flow shear $\Omega'\tau_A$. The flow shear required to stabilize the ballooning mode is smaller for the equilibria with an inside X-point than that for the outside one.

effect of toroidal shear flow through this mechanism, as well as raise the critical pressure gradient in a static plasma. In the equilibrium with inside X-point, the flow shear required to stabilize the ballooning mode is smaller than in the equilibrium with outside X-point. However, the critical pressure gradient is not largely changed by the modest flow shear.

Acknowledgements: I would like to thank Dr. Y. Kishimoto, Dr. M. Azumi, Dr. H. Shirai, Dr. T. Ozeki, Dr. M. Kikuchi, and Dr. A. Kitsunezaki for fruitful discussion and comments.

References

[1] J. W. Connor, Plasma Phys. Control. Fusion **40**, 531 (1998).
[2] F. Wagner, G. Becker *et al.*, Phys. Rev. Lett. **49**, 1408 (1982).
[3] L. L. Lao, Y. Kamada *et al.*, Nucl. Fusion **41**, 295 (2001).
[4] J. W. Conner, R. J. Hastie, and J. B. Taylor, Phys. Rev. Lett. **40**, 396 (1978).
[5] W. A. Cooper, Plasma Phys. Control. Fusion **30**, 1805 (1988).
[6] F. Pegoraro, Phys. Lett. A **142**, 384 (1989).
[7] E. Hameiri and S.-T. Chun, Phys. Rev. A **41**, 1186 (1990).
[8] K. Grassie and M. Krech, Phys. Fluids B **2**, 536, (1990), ibid, 1864, (1990).
[9] F. L. Waelbroeck and L. Chen, Phys. Fluids B **3**, 601 (1991).
[10] R. L. Miller, F. L. Waelbroeck *et al.*, Phys. Plasmas **2**, 3676 (1995).
[11] E. Frieman and M. Rotenberg, Rev. Mod. Phys. **32**, 898 (1960).
[12] M. Furukawa, Yuji Nakamura *et al.* , Phys. Plasmas **8**, 4889 (2001).
[13] H. P. Zehrfeld, B. J. Green, Nucl. Fusion **12**, 569 (1972).
[14] J. M. Greene and M. S. Chance, Nucl. Fusion **21**, 453 (1981).
[15] Y. Kamada *et al.*, Fusion Sci. Technol. **42**, 185 (2002).
[16] S. M. Kaye *et al.*, Sherwood Theory Conference, Rochester, N.Y. (2002).
[17] C. M. Bishop *et al.*, Nucl. Fusion **24**, 1579 (1984), ibid **26**, 1063 (1986).
[18] M. Azumi (private communication).